NASA TT F-11,572

SPACE AND TIME VARIATIONS IN THE LIGHT INTENSITY OF THE TWILIGHT SKY

T. G. Megrelishvili, T. I. Toroshelidze, and I. A. Khvostikov

Translation of: Prostranstvennyye i vremennyye variatsii intensivnosti svecheniya sumerechnogo neba
Bulletin of the Abastumani Astrophysical Observatory, No. 34, pp. 63-94, 1966

NATIONAL AERONAUTICS AND SPACE ADMINISTRATION
WASHINGTON, D.C. 20546 MAY 1968

SPACE AND TIME VARIATIONS IN THE LIGHT INTENSITY OF THE TWILIGHT SKY

T. G. Megrelishvili, T. I. Toroshelidze, and I. A. Khvostikov

ABSTRACT: The article represents a survey of the twilight data based upon our observations at Abastumani and those of other authors, carried out at different places, for different zenith distances and in various spectral regions.

Systematic measurements of the twilight sky have been made at /63* the Abastumani Astrophysical Observatory in various portions of the spectrum. The results of these measurements have been published in part [9, 10, 42, 43, 47, 55]. Since they are of interest for practical purposes (for example, for the characteristics of the illumination curve during twilight, etc.) as well as for a number of scientific problems in upper atmospheric physics, we shall present a comprehensive discussion of the aforementioned results in this paper. In addition to the observations made at the Abastumani Astrophysical Observatory, we shall also use data obtained by other investigators. This has permitted us to give a more final form to the discussion and to formulate certain conclusions in a more general manner.

Most of the measurements published for the brightness of the twilight sky have been made in relative rather than in absolute units, a fact that hinders comparison of data obtained by different authors. Therefore, in many cases, we also had to use relative units.

This survey consists of three parts. In the first, the introductory part, the general characteristics of the twilight sky are given from the photometric and spectrophotometric point of view. In the second part, a more detailed analysis is made of the spectral distribution of the brightness of the twilight sky as a function of the solar zenith distance in various seasons. Here, the morning and evening twilights are examined separately. In the third part, we discuss the results of studying the intensity variations of individual lines of the twilight glow in the atmosphere.

1. GENERAL CHARACTERISTICS OF THE RESULTS OF PHOTOMETRIC AND SPECTROPHOTOMETRIC STUDIES OF THE TWILIGHT SKY.

During the day, after noon, the day-sky brightness at the zenith decreases in proportion to the increase in the zenith distance

*Numbers in the margin indicate pagination in the foreign text.

(Z_0) of the sun, but at twilight, after sunset, the decrease is greatly accelerated. If we average the data of measurements from day-sky brightness at the zenith, made without light filters for various solar zenith distances, a curve will be obtained, according to Brunner's calculations [5] like that shown schematically in Figure 1. This curve explains the accepted division of twilight into three stages. The brightest part of twilight is called civil twilight ($Z_0 \leq 96°$). The darker part of twilight, when $96 \leq Z^0 \leq 102°$,

/64

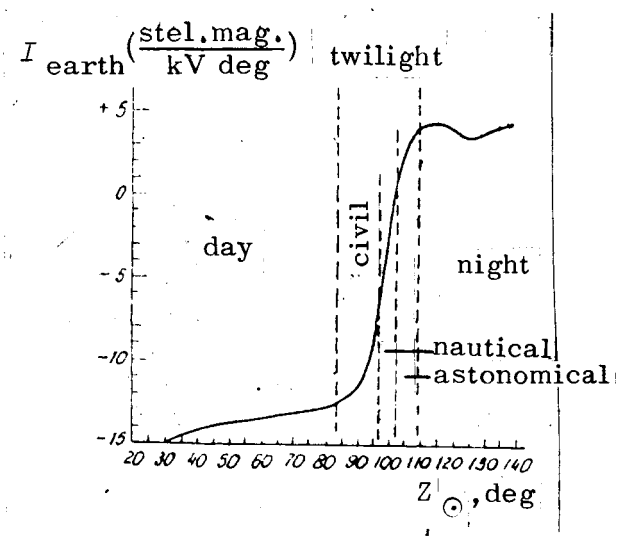

Fig. 1.

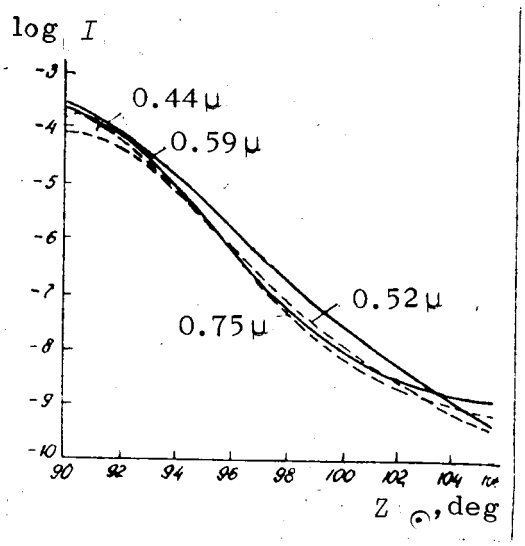

Fig. 2

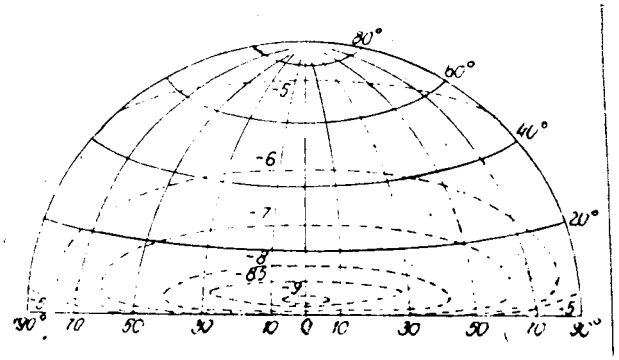

Fig. 3

is called nautical twilight; /65 up to the end of nautical twilight, it is still possible to distinguish reliably the line of the horizon. Nautical twilight is replaced by astronomical twilight which continues until the onset of night, when the rapid decrease in brightness of the sky ceases; this usually occurs when the solar zenith distance is about 2·5 lux; at the end of nautical twilight, it is about $6 \cdot 10^{-3}$ lux; and at the end of astronomical twilight, it decreases to $6 \cdot 10^{-4}$ lux [6].

At the beginning of twilight ($Z_0 = 90°$) the sun acquires a red coloration and the bright twilight band, whose color varies from orange-yellow at the bottom to green-blue at the top is stretched along the solar horizon. Above this band, there is a round, bright, almost colorless glow, while on the opposite side of the horizon, the bluish-grey dark segment of the Earth's shadow, edged with a pink band (Venus' girdle), slowly begins to rise.

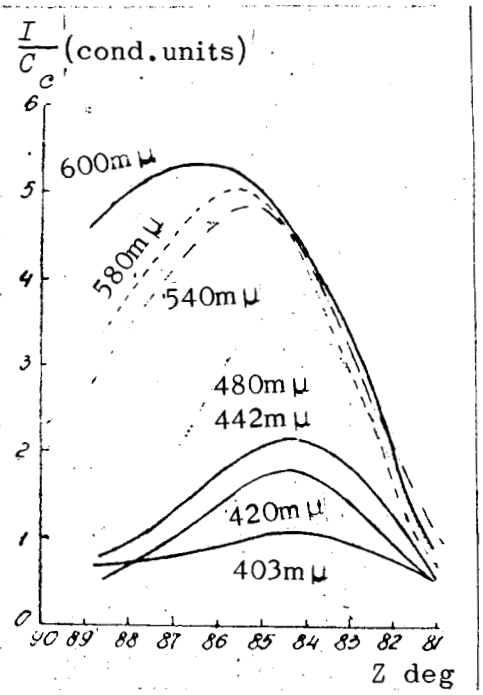

Fig. 4a.

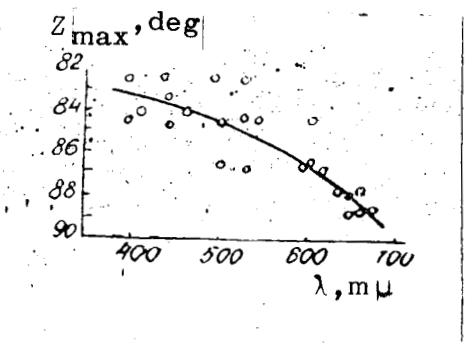

Fig. 4b.

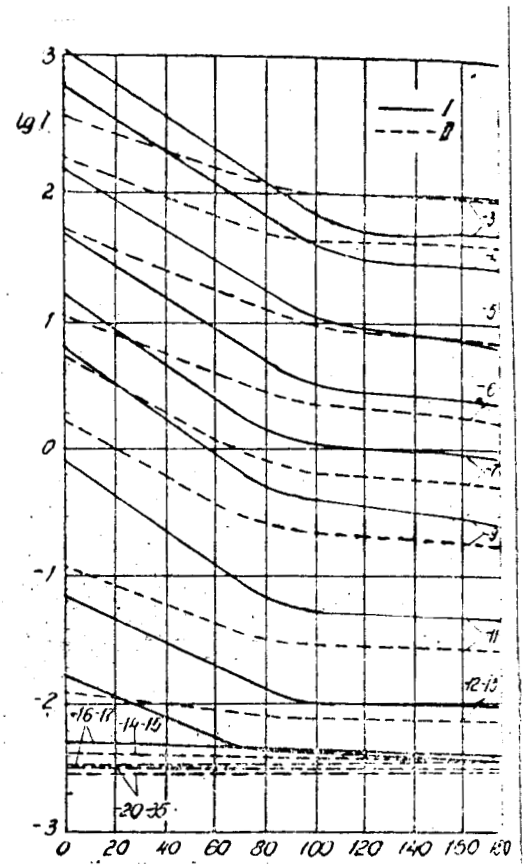

Fig. 5. Angle Between the Direction of the Sun and the Point of the Sky Observed, Deg.

/66

As the solar zenith distance increases, the color of the sky above the sun becomes more saturated and sometimes a purple light appears. This is a rose colored, rapidly diffusing spot, located at an elevation of 20-25° above the horizon.

At the end of civil twilight, the purple light fades and the multi-colored segment of the arch gradually contracts and becomes pale; at the beginning of astronomical twilight, it changes into a narrow, greenish-white band [3].

The pattern described is often observed in clear weather; when the atmosphere is turbid, the colors of the arch are more faded, and sometimes the glow phenomena simultaneously develop diversely in different portions of the sky [7].

A number of papers, especially the studies published by the workers at the Abastumani Astrophysical Observatory [8-10], have shown that the nature of the variation in the day-sky brightness as a function of the solar zenith distance varies substantially for different wavelengths, which may be the cause of serious errors in measurements involving broad portions of the spectrum [10]. Figure 2 presents the curves obtained by Eshborn with three interference light filters (λ_{eff} = 0.44, 0.52, and 0.59μ) having a half-width transmission band of 150 Å; the fourth light filter (0.75μ) had a half-width of 0.23μ [11].

The brightness distribution across the sky at twilight is far from being uniform. A bright portion of the sky is distinguished, viz., the comparatively small bright segment near the solar horizon. This is determined by the properties of light scattering under conditions where the atmosphere is illuminated from one side by the Sun from below the horizon. The isophots computed by N.M. Shtaude [12] (with allowance only for primary molecular scattering of light at Z = 90°) show such a bright spot in the sky at a small elevation above the horizon. According to Hurlburt's measurements [13], the dimensions of the bright segment decrease rapidly as the zenith distance increases. The position and the brightness of the bright spot is dependent on the wavelength. The measurements of A. Kh. Darchiya [14] give a detailed pattern of the brightness distribution in the bright segment. Figure 4 shows data for the instant that the Sun is on the horizon (Z = 90°), but a similar pattern holds even when the Sun is below the horizon (up to Z = 94°).

Measurements of the twilight-sky glow along various almucantars /67
show that changes in the brightness occur much more slowly along the azimuth than along the vertical.

Figure 5 shows the measurements of O.D. Boyarova [15] obtained by visual photometry without light filters.

2. SPECTRAL BRIGHTNESS DISTRIBUTION ACROSS THE TWILIGHT SKY.

The brightness of any portion of the sky during twilight varies rapidly as the solar zenith distance changes. Therefore, the so-called "twilight curves", i.e., the curves in Figure 2 should be considered the fundamental photometric characteristic of the twilight sky. It was shown in Part 1 that the shape of the twilight curves is dependent on the wavelength; it varies over the course of the year as well as between morning and evening twilights. In view of this, the most typical and reliable twilight curves, measured at different points of the sky, for different wavelengths, separately for different seasons and for morning and evening, are presented below in a systematic form for the characteristics of the spectral brightness distribution across the twilight sky. The completeness of the data presented is limited to published studies and unpublished measurements from the Abastumani Astrophysical Observatory.

TABLE 1

Zenith Distance of Sun $Z_{\odot}$;	Without filter; May 1947	Without filter; May 1948	Blue April - May 1948	Red April 1948
1	2	3	4	5
90°.0	2.024	2.162	1.390	0.867
5	1.905	2.050	1.289	0.757
91.0	1.768	1.916	1.155	0.632
5	1.621	1.765	1.012	0.491
92.0	1.458	1.597	0.849	0.330
5	1.270	1 407	0.675	0.149
93.0	1.074	1.199	0.478	9.944
5	0.863	0.984	0 266	9.713
94.0	0.642	0.757	0.042	9.462
5	0.409	0.521	9.806	9.189
95.0	0.167	0.269	9.561	8.905
5	9.924	0.012	9.305	8.617
96.0	9.669	9.752	9.043	8.322
5	9.413	9.483	8.779	8.025
97.0	9.154	9.208	8.518	7.734
5	8.903	8.916	8.244	7.447
98 0	8.653	8.677	7.983	7.143
5	8.422	8.449	7.75	
99.0	8.195	8.241	7.513	
5	7.991	8.037		
100.0	7.783	7.842		
5	7.579	7.644		
101.0	7.379	7.451		
5	7.379	7.268		
102.0		7.077		

2.1. Twilight Curves Measured at the Zenith for Different Wavelengths.

Table 1 shows twilight curves (in relative units) from measurements [16] with two light filters, viz., a blue filter (centered at 0.435μ) and a red filter (0.635μ); a twilight curve without a light filter is given for comparison. This latter curve, with allowance for the spectral sensitivity of the photomultiplier (the measurements

were made photoelectrically), corresponds to an effective wavelength of 0.46μ.

A comparison of the figures in the next-to-last and last columns of this table clearly shows the effect of the "blueing" of the twilight sky (at the zenith) with increasing zenith distance of the sun during civil twilight. In fact, the brightness of the sky decreases, with solar zenith distance, more rapidly in the red light filter than in the blue light filter; if the ratio of the brightness is $J_{blue}/J_{red} = 3.3$ for a zenith distance of 90-91.5° (this follows from the fact that $\log J_{blue} - \log J_{red} = 0.52$), then for a zenith distance of 94°, the ratio increases to 3.8, for a zenith

/68

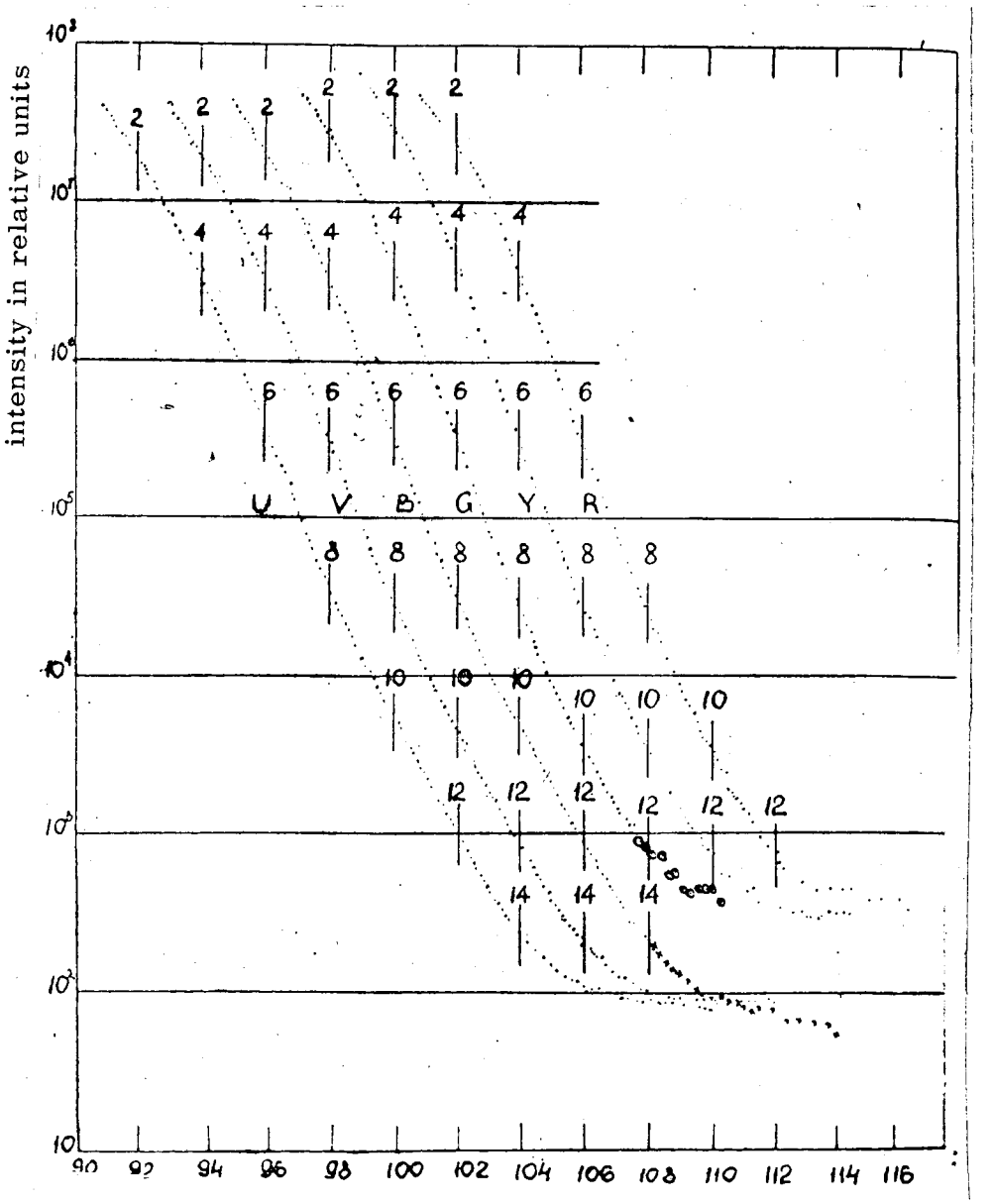

Fig. 6.

distance of 96°, it is 5.2, and for a zenith distance of 98°, it increases to 6.9.

A fuller and more detailed pattern of the dependencies of the twilight curves is given by the measurements of Dave and Ramanathan in India [17] with six filters having the following transmission bands: /69

U	0.33 — 0.380 μ
V	0.364 — 0.405,
B	0.435 — 0.480,
G	0.553 — 0.575,
Y	0.58 — 0.60,
R	0.60 — 0.64.

Here the intensities are given in relative units. The measurements were made in the evening. Figure 6 shows curves averaged for 2-3 days as follows:

Light filter *U* - average for three days (20-22 September 1951)
" *V* " " " " (30 September and 1 and 22 November 1951)
" *B* - (23 October 1951)
" *G* - average for 2 days (23 and 28 September 1951)
" *Y* - " " 4 " (19-22 September 1951)
" *R* - " " 2 " (29 September and 1 November 1951).

To this point, we have examined measurements in the visible portion of the spectrum. Measurements in the infrared region have been made at the Abastumani Observatory. Table 2 presents mean-monthly values for different seasons, separately for the morning and evening twilights.

For purposes of comparison, Table 3 gives analogous measurements, made synchronously at the Abastumani Observatory in the blue portion of the spectrum (0.533μ).

2.2. The Spectral Distribution of the Day-Sky Brightness Along The Vertical of the Sun. /70

Table 4 gives values of the day-sky brightness as measured in Switzerland [16] during 1947 at different points of the vertical of the Sun on a wavelength of 0.635μ; the measurements were made photoelectrically. In this table, the rows are for different values of solar zenith distances, while the columns are for the different values of the zenith distance of that point in the sky at which the measurements were made. The data are given in relative units (the value of the luminosity *J* for the zenith is taken everywhere as the unit). Positive Z are the lines of vision directed toward the solar horizon (the west in the evening) and the negative are for the opposite direction (the east in the evening). The table gives

TABLE 2.

zenith distance of sun Z⊙ \ Month	Aug.	Sept.		Oct.	Nov.		Dec.	Feb.	March		July	
	even	morn	even	even	morn	even	even	even	morn	even	morn	even
95°.0	2.75	2.41	1.96	2.06	1.72	2.28	2.37	1.83		2.14	2.15	1.9
.6	2.50	2.12	1.67	1.71	1.39	1.69	2.06	1.50		1.72	1.80	1.5
96.0	2.13	1.95	1.46	1.50	1.34	1.38	1.86	1.30	2.74	1.45	1.55	1.3
.6	1.73	1.72	1.19	1.28	1.12	1.07	1.66	0.91	2.22	1.12	1.18	0.9
97.0	1.53	1.56	1.01	1.09	0.92	0.93	1.51	0.67	1.90	0.88	0.98	0.7
.6	1.26	1.39	0.81	0.90	0.71	0.72	1.33	0.38	1.53	0.60	0.71	0.5
98.0	1.09	1.22	0.65	0.72	0.53	0.50	1.20	0.23	1.26	0.37	0.52	0.3
.6	0.87	1.05	0.54	0.50	0.34	0.27	1.00	0.03	0.95	0.11	0.33	0.1
99.0	0.71	0.92	0.36	0.30	0.18	0.10	0.88	−0.10	0.72	0.05	0.23	1.0
.6	0.50	0.72	0.11	0.08	−0.02	−0.09	0.70	−0.26	0.40	0.22	0.04	−0.0
100.0	0.33	0.58	−0.04	−0.08	0.11	0.16	0.58	0.36	0.14	0.32	−0.08	0.2
.6	0.12	0.42	0.04	0.26	0.25	0.28	0.46	0.47	−0.10	0.42	0.32	0.4
101.0	0.07	0.26	0.37	0.40	0.38	0.34	0.35	0.52	0.28		0.49	0.5
.6	0.22	0.02	0.54	0.52	0.42	0.40	0.22		0.48		0.68	
102.0	0.30	0.14		0.61			0.13		0.60		0.70	
.6	0.38						0.03					

TABLE 3.

zenith distance of sun Z⊙ \ Month	Aug.	Sept.		Oct.	Nov.		Dec.	Feb.	March	
	even	morn	morn	even	morn	even	even	even	morn	even
95°.0	3.90	4.12	3.82	3.88	3.14	3.81	3.92	3.97		4.01
.6	3.60	3.77	3.55	3.56	2.89	3.48	3.60	3.68		3.61
96.0	3.39	3.57	3.29	3.32	2.68	3.23	3.36	3.40		3.32
.6	3.08	3.38	3.00	3.05	2.40	2.86	3.66	3.04	3.93	3.23
97.0	2.87	3.08	2.79	2.83	2.18	2.56	2.92	2.72	3.51	2.75
.6	2.57	2.70	2.50	2.57	1.95	2.26	2.66	2.38	3.08	2.42
98.0	2.35	2.58	2.29	2.37	1.70	2.07	2.51	2.10	2.78	2.20
.6	2.07	2.27	2.00	2.11	1.40	1.82	2.17	1.83	2.30	1.92
99.0	1.89	2.16	1.80	1.90	1.19	1.65	1.95	1.63	2.00	1.75
.6	1.61	1.83	1.55	1.66	0.96	1.36	1.66	1.40	1.70	1.50
100.0	1.32	1.63	1.38	1.46	0.86	1.16	1.45	1.22	1.47	1.31
.6	1.16	1.38	1.18	1.25	0.73	1.00	1.28	1.00	1.22	1.14
101.0	0.99	1.21	1.03	1.05	0.61	0.88	0.96	0.86	1.06	1.00
.3	0.89	1.00	0.85	0.86	0.51	0.73	0.82	0.71	0.84	0.82
102.0	0.69	0.87	0.72	0.76	0.45	0.66	0.71	0.57	0.60	0.75
.6	0.70				0.36		0.56	0.45	0.38	0.61
103.0							0.42	0.34		0.29

the mean annual values.

/71

TABLE 4.

Vertical of the sun Z / $Z_\odot$	+75°	+60°	+45°	+30°	0°	−30°	−45°	−60°	−75°
90°.0	8.79	4.26	2.59	1.47	1	1.29	1.76	2.63	4.02
.5	8.21	3.95	2.84	1.46	1	1.25	1.75	2.54	3.77
91.0	8.21	3.89	2.26	1.44	1	1.32	1.78	2.45	3.53
.5	8.28	8.97	2.28	1.46	1	1.31	1.78	2.47	3.43
92.0	8.81	4.23	2.33	1.50	1	1 33	1.76	2.46	3.10
.5	9.46	4.39	2.38	1.49	1	1.28	1 68	2.33	2.63
93.0	10.2	4.60	2.45	1.51	1	1.22	1.55	2.15	2.31
.5	11.7	5.07	2.65	1.54	1	1.17	1.50	1.95	2 06
94.0	13.4	5.87	3.02	1.68	1	1.17	1.44	1.83	1.79
.5	16.4	6.17	3.17	1.64	1	1.19	1.43	1.76	1.62
95.0	16.4	6.07	3.05	1.60	1	1.26	1.45	1.76	1.67
.5	15.7	6.03	3.01	1.63	1	1.32	1.46	1 79	1.74
96 0	16.0	6.33	3.04	1.66	1	1.31	1.45	1.82	1.81
.5	16.5	6.44	3.13	1.72	1	1.32	1.46	1.91	1.92
97.0	15.7	6.29	3.05	1.72	1	1.26	1.36	1.89	1.97
.5	15.5	6.11	2.93	1.71	1	1.19	1.27	1.88	2.01
98.0	14.5	5.78	2.76	1.60	1	1.11	1.15	1.84	2.03

Table 5 presents similar data for a shorter wavelength, viz., 0.528μ. It should be noted that for this wavelength also, the day-sky brightness is concentrated close to the solar horizon (Z = 75°), but, in comparison with 0.635μ, the brightness distribution along the Sun's vertical is more uniform; for example, for $Z_\odot$ = 94°, the brightness at the point of the vertical Z = 75° for 0.528 exceeds the brightness at the zenith only by a factor of 10.6 (J_{+75}/J_0=10.6),

TABLE 5.

Z / $Z_\odot$	+75°	+60°	+45°	+30°	0°	−30°	−45°	−60°	−75°
90°.0	6.90	3.89	2.22	1.49	1	1.35	1.77	2.61	3.37
.5	6.81	3.90	2.25	1.50	1	1.32	1.75	2.51	3.16
91.0	6.91	3.95	2.31	1.47	1	1.30	1.75	2.37	2.87
.5	7.33	3.98	2.27	1.46	1	1.29	1.70	2.25	2.60
92.0	7.82	4.02	2.28	1.45	1	1.27	1.61	2.14	2.30
.5	8.06	4.03	2.23	1.45	1	1.22	1.55	1.93	1.96
93.0	8.64	4.25	2.31	1.46	1	1.21	1.52	1.81	1.71
.5	9.52	4.57	2.50	1.50	1	1.19	1.52	1.70	1.61
94.0	10.6	4.83	2.66	1.57	1	1.20	1.47	1.69	1.59
.5	11.0	4.81	2.66	1.60	1	1.18	1.40	1.63	1.58
95.0	11.0	4.77	1.60	1.57	1	1.11	1.33	1.51	1.55
.5	11.5	4.98	2.70	1.59	1	1.11	1.31	1.42	1.59
96.0	12.2	5.22	2.78	1.63	1	1.08	1.29	1.41	1.71
.5	12.9	5.53	2.88	1.70	1	1.10	1 30	1.49	1.86
97.0	14.0	6.01	3.06	1.82	1	1.16	1.40	1.77	2.05
.5	14.9	6.38	3.17	1.92	1	1 32	1.52	1.95	2.39
98.0	16.2	6.92	3 26	2.01	1	1.46	1 68	2 30	2.81
.5	16.4	6.97	3.31	1.98	1	1.52	1.76	2.50	3.08
99.0	16.3	7.02	3.27	1.95	1	1.55	1.87	2.73	3.37

while, for wavelength 0.635, this ratio is equal to 13.4. But this effect occurs only up to $Z_\odot$ = 96.5°, where this ratio has values of 12.9 and 16.5, respectively. For greater depressions of the sun below the horizon, the ratio J_{+75}/J_0 continues to increase for wavelength 0.528μ (for $Z_\odot$ = 98° it is equal to 16.2), while for wavelength 635μ, the ratio decreases (to 14.5 for $Z_\odot$ = 98°).

However, for even greater $Z_\odot$, a change in the increase of that ratio as a function of $Z_\odot$ is also observed for wavelength 0.528μ (compare, for example, the values of J_{+75} for $Z_\odot$ = 98°.0 and for

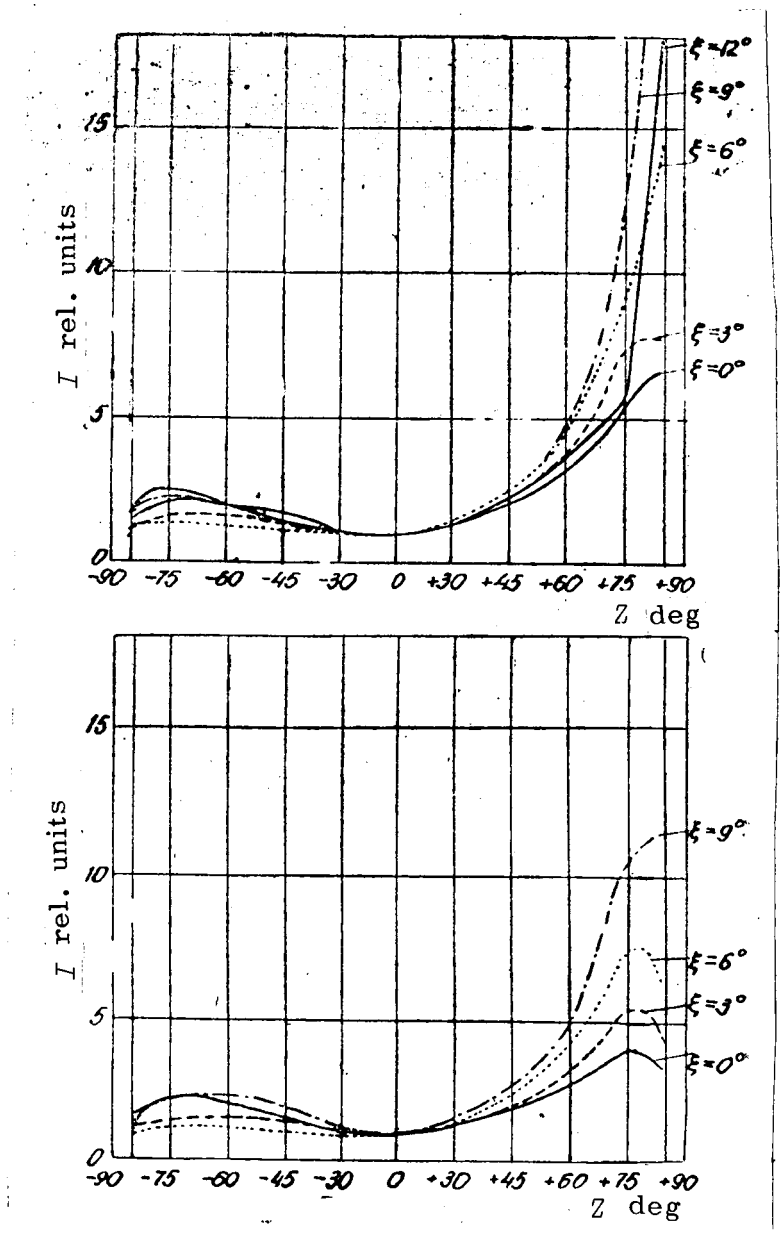

Fig. 7a, b.

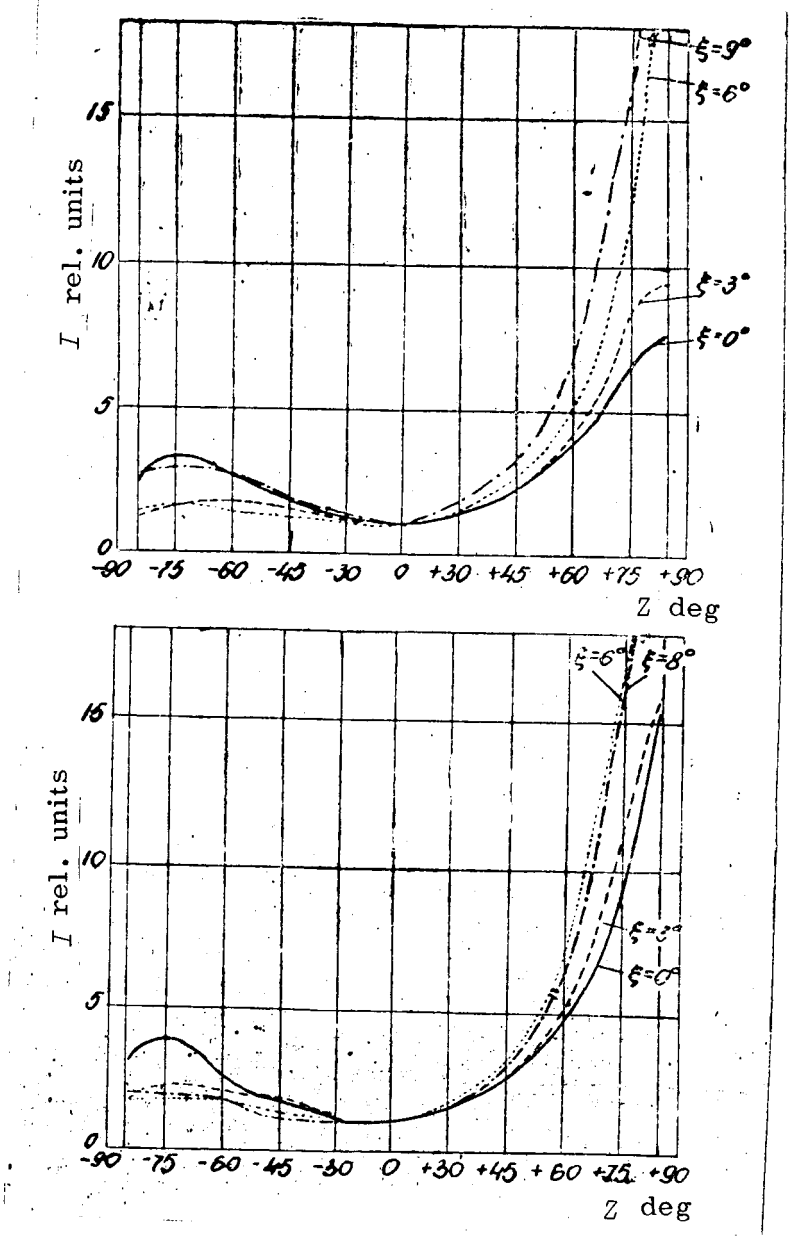
I rel. units
15
10
5
0
ξ=9°
ξ=6°
ξ=3°
ξ=0°
-90 -75 -60 -45 -30 0 +30 +45 +60 +75 +90
Z deg
I rel. units
15
10
5
0
ξ=6°
ξ=8°
ξ=3°
ξ=0°
-90 -75 -60 -45 -30 0 +30 +45 +60 +75 +90
Z deg

Fig. 7c, d.

98.5° in Table 5). /74

TABLE 6.

$Z_\odot$ \ Z	+75°	+60°	+45°	+30°	0°	−30°	−45°	−60°	−75°
90°.0	4.19	2.89	2.04	1.30	1	1.23	1.63	2.03	2.25
.5	4.64	3.14	2.05	1.38	1	1.26	1.67	2.09	2.18
91.0	4.87	3.21	2.04	1.38	1	1.26	1.62	2.04	2.05
.5	5.13	3.23	2.03	1.36	1	1.24	1.57	1.91	1.80
92.0	5.17	3.27	2.03	1.38	1	1 20	1.49	1.74	1.65
.5	5.42	3.20	2.02	1.39	1	1.17	1.45	1.60	1.47
93.0	5.55	3.28	2.07	1.41	1	1.20	1.44	1.55	1.41
.5	5.66	3.46	2.13	1.45	1	1.17	1.40	1.55	1.33
94.0	5.82	3.51	2 24	1.51	1	1.14	1.36	1.55	1.29
.5	6.02	3.57	2.27	1.48	1	1.13	1.31	1.40	1.25
95.0	6.26	3.66	2.26	1.46	1	1.12	1.24	1.27	1.23
.5	6.71	3.88	2.35	1.51	1	1.09	1.18	1.24	1.20
96.0	7.51	4.16	2.44	1.48	1	1.03	1.13	1.21	1.14
.5	8.29	4.49	2.58	1.58	1	1.09	1.25	1.40	1.33
97.0	8.89	4.64	2 64	1.74	1	1.14	1.39	1.59	1.58
.5	9.51	4.87	2.73	1.77	1	1.23	1.58	1.80	1.79
98.0	10.3	5.04	2.82	1.58	1	1.31	1.76	2.04	1.97
.5	10.5	4.99	2.76	1.83	1	1.34	1.87	2.18	2.06
99.0	10.5	4.79	2.65	1.80	1	1.32	1.96	2.32	2.11

If we look at similar measurements for a still smaller wavelength (0.435μ; Table 6), such comparisons show that there are similar regularities for the shortwave end of the visible spectrum also: the brightness distribution along the vertical of the Sun is even more uniform ($J_{+75}/J_\odot$ = 5.28 for $Z_\odot$ = 94° and 8.29 for 96.5°), but the ratio ceases to increase for greater $Z_\odot$ (see the values for 98.5° and 99° in Table 6). This latter fact is related to distinctive variations in the spectral composition of the illumination from the bright segment, a subject that will be mentioned in detail below (see Sections 2 and 3). Different regularities are characteristic for the brightness distribution in the Sun's vertical on the other side of the zenith, as the numbers in the last column of Tables 4-6 show.

The graphs in Figure 7 give a clear idea of the aforementioned properties of the brightness distribution along the Sun's vertical. These curves were taken from a paper written by the author of [16]. They are for different depressions of the Sun below the horizon (the value of $Z_\odot$ =-90° is shown near each curve). The data here are also given in relative units (J = 1 is taken for the zenith). The graphs are also plotted for the wavelengths 0.635 (Fig. 7d), /75
0.528 (Fig. 7c), and 0.435μ (Fig. 7b) as well as for measurements without a light filter (Fig. 7a); in the last case, allowance was made for the spectral sensitivity of the apparatus (λ_{eff} was taken to be equal to 0.46μ).

Up to this point, we have examined the day-sky brightness distribution along the vertical of the sun in relative units. The absolute values of the twilight sky brightness at various points are,

of course, of great interest. Such measurements have been made at the Astrophysical Institute of the Academy of Sciences of the Kazakh SSR (the Kamenskoye Plateau, near Alma-Ata), using a photoelectric photometer [18]. The measurements were made with two interference light filters, centered at 0.371 and 0.576μ (the half-width transmission bands of the light filters was 165 Å and 74 Å, respectively). The results, obtained in April 1959, are given in Table 7 (for 0.371) and Table 8 (for 0.576). The tables give the values in millionths (see the factor 10^{-6} in the last column) of erg/cm^{2}sec Å degrees.

TABLE 7.

$Z_\odot$ \ Z	+75°	+60°	+40°	+30°	0°	−30°	−40°	−60°	−75°	factor
94°	22	16	11	8.3	6.1	6.6	7.2	7.6	6.2	10^{-6}
95	8.4	6.5	4.0	3.1	2.1	2.4	2.5	2.6	2.4	10^{-6}
96	38	25	15	11	7.3	7.9	8.5	9.3	8.8	10^{-7}
97	15	9.0	5.0	3.9	2.5	2.7	2.9	3.5	3.5	10^{-7}
98	51	32	16	14	8.8	9.9	11	14	14	10^{-8}
99	18	11	6.1	5.0	3.3	3.9	4.5	6.2	5.5	10^{-8}
100	6.1	3.9	2.5	2.0	1.4	1.7	1.9	2.4	2.1	
101	22	16	10	8.5	6.0	6.9	8.1	9.7	8.7	10^{-9}
102	8.5	6.6	4.4	3.7	2.7	3.1	3.5	4.2	3.7	10^{-9}
103	3.7	2.9	1.9	1.7	1.2	1.4	1.6	1.8	1.6	10^{-9}
104	17	14	9.9	8.9	6.1	7.0	7.6	7.9	7.5	10^{-10}

TABLE 8.

93°	46	20	11	8.0	4.7	5.5	6.6	8.6	8.2	10^{-6}
94	16	7.9	4.1	3.0	1.7	2.1	2.3	3.0	2.5	10^{-6}
95	54	26	12	8.3	5.0	5.5	6.1	7.1	6.4	10^{-7}
96	18	8.2	3.6	2.4	1.4	1.3	1.6	1.7	1.9	10^{-7}
97	69	21	9.8	6.8	3.7	4.1	4.3	5.6	6.7	10^{-8}
98	24	8.7	3.1	2.1	1.1	1.3	1.4	2.0	2.6	10^{-8}
99	84	24	10	6.9	4.1	4.5	5.3	7.8	10	10^{-9}
100	29	8.5	3.5	2.8	1.9	2.1	2.4	3.5	4.8	10^{-9}
101	100	34	16	13	9.8	11	12	17	22	10^{-10}
102	41	19	10	7.8	6.5	7.3	7.5	10	11	10^{-10}
103	19	11	6.2	5.2	4.4	4.8	4.9	6.3	6.9	10^{-10}
104	12	6.3	4.3	3.7	3.0	3.5	3.7	4.5	5.0	10^{-10}

2.3. The Brightness Distribution in the Bright Segment.

The special features of the spectral composition of the illumination of the bright segment have already been mentioned above. This problem deserves a comprehensive study, all the more since the day-sky brightness is concentrated into the comparatively small bright segment. Extensive studies of this kind have been made by A. Kh. Darchiya [14]. Some of her results are given in Figure 4. The spectra of this part of the twilight sky are seen to be extremely diverse, a fact that is easily explained, since the measurements were made near the horizon where they are quite sensitive to even slight variations in the optical characteristics of the atmosphere (extinction, aerosol scattering). Figure 8 shows examples of the spectral dependencies of the day-sky brightness (in units of day-

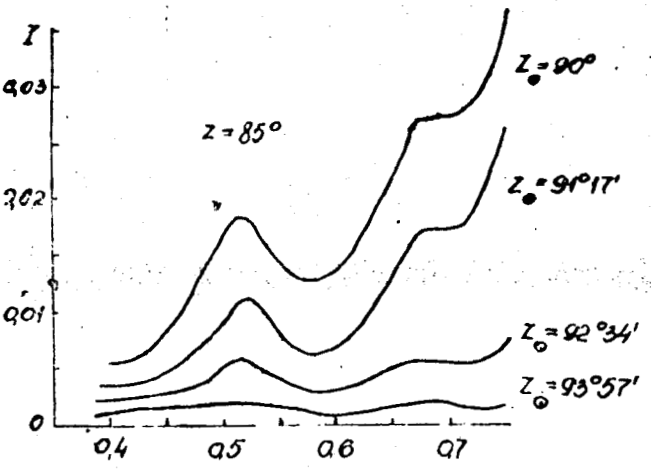

Fig. 8.

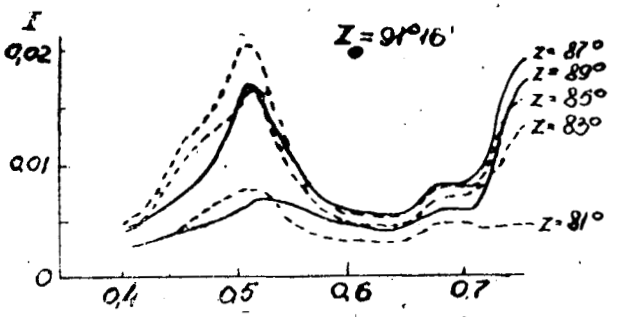

Fig. 9.

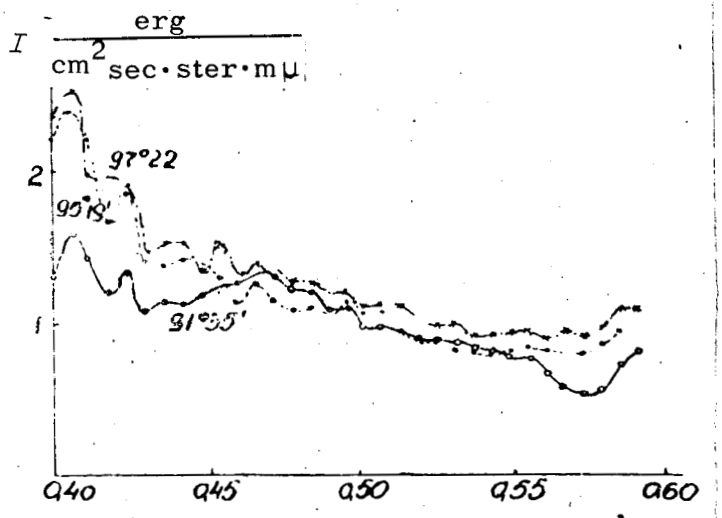

Fig. 10.

time illumination) in the bright segment for various solar zenith distances. The spectra clearly show the Shapnyui ozone absorption band between 0.5 and 0.7 , although it varies greatly from day to day. But the unit selected for the measurements (the day-time luminosity of a horizontal white screen) disrupted the spectral behavior of the curves in Figure 8 because the spectrum of day-time illumination differs greatly from the spectrum of the Sun. /77

Figure 9 gives examples of the spectral dependencies of the day-sky brightness also in units of day-time illumination in the bright segment for different zenith distances of the line of vision Z for $Z_\odot = 91°16'$ [14]. A comparison of the curves in Figures 8 and 9 shows that the Shapnyui band appears more clearly, the closer to the horizon the spectrum is taken.

The absorption of light by atmospheric ozone has an important effect on the color of the twilight sky [20-22]. Coody and Volz [19] calculated in detail the spectral curve of the day-sky brightness in the solar vertical at point Z = 70° (with allowance only for single scattering) and at a solar zenith distance of 90° in the region of the Shapnyui band for a purely molecular atmosphere (Curve in Figure 11) and for an atmosphere containing aerosols (Curve D).

TABLE 9.

$Z_\odot$	without filter		blue	red
	1917 May	1948 May	1948 Apr–May	1948 April
90°.0	2.021	2.162	1.390	0.867
.5	1.905	2.050	1.289	0.757
91.0	1.768	1.916	1.155	0.632
.5	1.621	1.765	1.012	0.491
92.0	1.458	1.597	0.849	0.330
.5	1.270	1.407	0.675	0.149
93.0	1.074	1.199	0.478	9.944
.5	0.863	0.984	0.256	9.713
94.0	0.642	0.757	0.042	9.462
.5	0.409	0.521	9.806	9.189
95.0	0.167	0.269	9.561	8.905
.5	9.924	0.012	9.305	8.617
96.0	9.669	9.752	9.043	8.322
.5	9.413	9.483	8.779	8.025
97.0	9.154	9.208	8.518	7.734
.5	8.903	8.916	8.244	7.447
98.0	8.653	8.677	7.983	7.143
.5	8.422	8.449	7.75	
99.0	8.195	8.241	7.513	
.5	7.991	8.073		
100.0	7.783	7.842		
5	7.579	7.644		
101.0	7.379	7.451		
.5	7.379	7.268		
102.0		7.077		

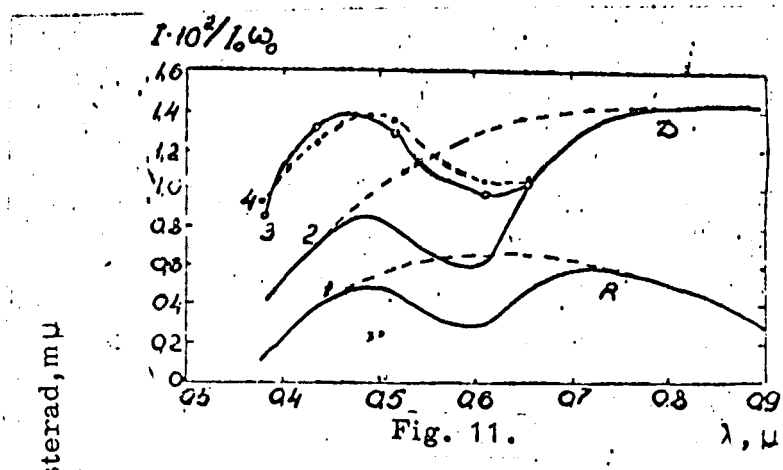

Fig. 11.

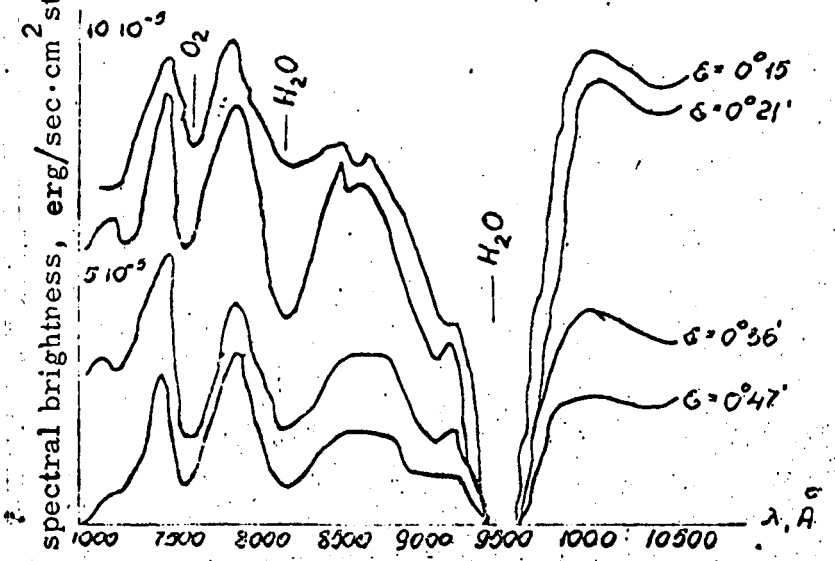

Fig. 12.

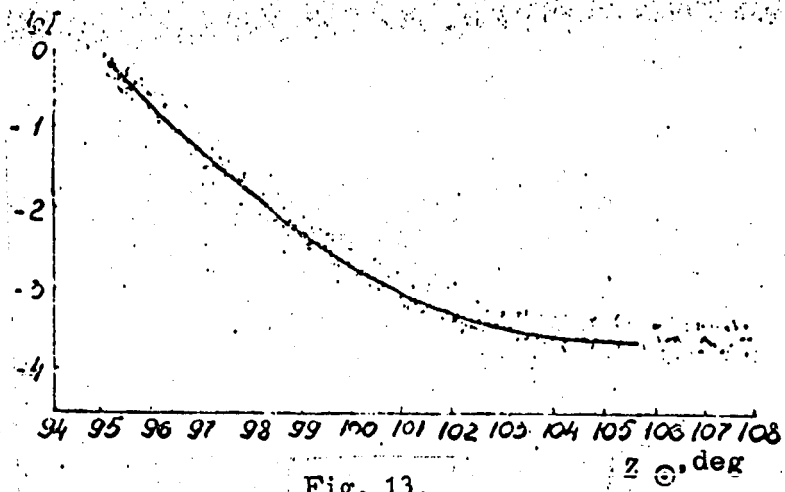

Fig. 13.

The same figure presents the results of their luminosity measurements with interference light filters for two days (Curves 3 and 4) with the solar zenith distance equal to 90°.

2.4. Spectra of the Twilight Sky at the Zenith.

Reference [8] employed a fast f:1 spectrograph to obtain a number of spectra at the zenith for different solar zenith distances. It was possible to establish the nature of the variations in the spectral composition of the scattered light of the twilight sky as a function of the solar zenith distance (these curves will be examined in Section 2.6, see Figure 14). The measurements in absolute units made by I.M. Mikhailin, G.V. Rozenberg, et al, the results of which are shown in Figure 10, are of great interest (curve 1 is for 91°35', curve 2 is for 95°19', and curve 3 is for 97°22'). The numbers on the ordinate must be multiplied by 10^{-5} (curve 1), 10^{-7} (curve 2), or 10^{-8} (curve 3). In monograph [3], curves similar to those shown in Figure 10, but measured in units of solar brightness, can be found. /79

Observations of the spectra of the twilight sky [23] in the 0.55-0.66μ region were made in Yakutsk in 1961 (with the fast SP-48 spectrograph).

TABLE 10.

$Z_\odot$	without light filter	0.435 мк	0.528	0.635
	July–Aug.	July–Aug.	July–Aug.	July–Aug.
90°.0	2.177	1.357	1.240	0.830
.5	2.071	1.236	1.129	0.795
91.0	1.948	1.103	1.001	0.696
.5	1.807	0.966	0.860	0.576
92.0	1.652	0.809	0.705	0.438
.5	1.471	0.636	0.533	0.286
93.0	1.268	0.438	0.332	0.109
.5	1.038	0.226	0.100	9.892
94.0	0.806	9.992	9.847	9.639
.5	0.566	9.749	9.589	9.365
95.0	0.307	9.492	9.332	9.077
.5	0.046	9.241	9.064	8.791
96.0	9.780	8.981	8.790	8.507
.5	9.511	8.715	8.519	8.221
97.0	9.248	8.457	8.245	7.956
.5	8.994	8.191	7.977	7.698
98.0	8.746	7.429	7.712	7.445
.5	8.512	7.697	7.469	
99.0	8.303	7.472	7.229	
.5	8.105			
100.0	7.901			
.5	7.703			
101.0	7.511			
.5	7.321			
102.0	7.131			

Figure 12 reproduces the infrared spectra of the twilight sky as measured in the summer of 1963 at Pulkova in absolute units [24]. The aperture ratio of the monochromator was f:9 and the dispersion was 22 Å per mm. The energy distribution curves showed the strongest O_2 and H_2O absorption bands. The curves were measured for different depressions of the Sun below the horizon and $Z_\odot$ was -90°. /80

2.5. Distribution of the Spectral Brightness Across the Twilight Sky in Various Seasons.

It has been established that there are seasonal variations which characterize the spectral composition of the twilight sky at its various points. Tables 9 and 10 present measurements made [16] in 1947-1948 during the spring (April-May, Table 9) and at the end of summer (July-August, Table 10) with different light filters, centered at 0.435μ (blue), 0.528μ (green), and 0.635μ (red). The measurements were made at the zenith; the results are shown in relative units (the tables give the values of the logarithms of brightness).

TABLE 11.

$Z_\odot$ \ Z	+75°	+60°	+45°	+30°	0°	−30°	−45°	−60°	−75°
90°.0	6.73	3.72	2.25	1.50	1	1.40	1.79	2.55	3.32
.5	6.61	3.69	2.24	1.47	1	1.30	1.76	2.43	3.13
91.0	7.12	3.78	2.23	1.47	1	1.28	1.76	2.36	2.95
.5	7.33	3.82	2.23	1.44	1	1.26	1.66	2.18	2.68
92.0	7.48	3.92	2.23	1.43	1	1.25	1.59	2.02	2.34
.5	7.31	3.86	2.15	1.38	1	1.26	1.56	1.90	2.01
93.0	7.26	7.55	2.04	1.34	1	1.14	1.43	1.63	1.73
.5	6.99	3.20	1.92	1.31	1	1.08	1.31	1.54	1.46
94.0	8.18	3.96	2.03	1.34	1	1.11	1.48	1.68	1.45

TABLE 12.

$Z_\odot$ \ Z	+75°	+60°	+45°	+30°	0°	−30°	−45°	−60°	−75°
90°.0	9.65	4.94	2.72	1.59	1	1.45	1.89	2.69	4.17
.5	9.37	4.64	2.67	1.60	1	1.39	1.84	2.66	3.91
91.0	9.30	4.55	2.65	1.59	1	1.33	1.81	2.59	3.63
.5	9.18	4.45	2.60	1.54	1	1.23	1.73	2.46	3.28
92.0	8.89	4.22	2.45	1.49	1	1.21	1.64	2.20	2.54
.5	8.64	3.95	2.28	1.40	1	1.19	1.54	1.91	1.25
93.0	8.50	3.63	2.11	1.38	1	1.23	1.45	1.70	1.94
.5	7.42	3.39	1.87	1.24	1	1.23	1.39	1.54	1.63
94.0	8.27	3.70	1.98	1.33	1	1.18	1.20	1.32	1.42

Tables 4-6 in Section 2.2. presented data [16] on the mean annual distribution of brightness along the vertical of the sun. This same paper gave similar data, but for the individual months: for December-January [16] gave similar data, but for the individual months: for December-January (0.528μ, Table 11; 0.635μ, Table 12) and for April-May (0.435μ, Table 13; 0.635μ, Table 14). A compari-

son between Table 11-14 and Tables 4-6 permits the existence of marked seasonal variations in the brightness distribution to be established.

Extensive data, permitting a judgment to be formed on certain regularities of the seasonal variations, were obtained at the Abastumani Astrophysical Observatory. These data encompassed various portions of the visible spectrum and the infrared spectrum. Table 2 (see Section 2.1.) gives measurements in the infrared region: the mean-monthly values of the logarithms of brightness are shown in relative units. The observations were made with a photoelectric photometer through a light filter centered at 0.94μ; the transmission band of the light filter had a half-width of 0.14μ. /81

TABLE 13.

Z / $Z_\odot$	+75°	+60°	+45°	+30°	0_o	−30°	−45°	−60°	−75°
90°.0	4.78	3.18	2 12	1.43	1	1.26	1.69	2.38	2.50
.5	4.89	3.15	2.03	1.42	1	1.24	1.67	2.35	2.32
91.0	5.01	3.16	2 09	1.43	1	1.26	1.66	2.24	2.22
.5	5.19	3.30	2.08	1.43	1	1.28	1.52	2.53	2.04
92 0	5.29	3.28	2.09	1.43	1	1.27	1.58	1.96	1.81
.5	5.30	3.11	2.03	1.42	1	1.21	1.57	1.78	1.70
93.0	5.28	3.28	2.11	1.43	1	1.18	1.50	1.70	1.41
.5	5.34	3.33	2.11	1.44	1	1.14	1.43	1.59	1.32
94.0	5.58	3.40	2.19	1.49	7	1.11	1.37	1.50	1.26
.5	5.89	3.53	2.27	1.50	1	1.09	1.33	1.43	1.21
95.0	6.41	3 70	2.32	1.53	1	1.07	1.28	1.37	1.22
.5	7.03	3.92	2.42	1.55	1	1.05	1.24	1.36	1.31
96.0	7.89	4.24	2.51	1.61	1	1.03	1.25	1.36	1.43
.5	8.67	4.49	2.57	1.63	1	1.02	1.21	1.35	1.52
97.0	9.72	4.71	2.67	1.71	1	1.04	1.31	1.53	1.68
.5	11.0	5.03	2 83	1.82	1	1.12	1.50	1.77	1.89
98 0	12.5	6.40	2.98	1.93	1	1.25	1.74	1.99	2.10
.5	12.9	5.23	2.86	1.90	1	1.26	1.83	2.08	2.13
99.0	13.5	5.15	2.75	1.86	1	1 27	1.94	2.17	2.17

Measurements were made simultaneously in the visible region of the spectrum. Table 15 gives the same data for 0.64μ (the width of the transmission band of the light filter was 0.11μ) and Table 3 (see Section 2.1) gives data for 0.533μ (the transmission band was 0.12μ).

An analysis of the seasonal variations and the reasons behind them produces a complex and inadequately studied problem if we refer to the quantitative theory of the corresponding processes. But four basic groups of processes can be pointed out.

1. The seasonal changes in the structure of the atmosphere (the vertical distribution of temperature, density, etc.), which are accompanied by corresponding changes in its optical characteristics.

2. Seasonal variations in the turbidity of the atmosphere, including its high layers, which strongly affects the scattering power of various layers and, therefore, the brightness and spectral composition of the background of the twilight sky.

3. Seasonal variations of the ozone content.

4. The luminosity of the upper layers of the atmosphere depends, among other factors, on the degree of dissociation, the ionization of various components of the atmosphere (especially oxygen), and the rate of many chemical (photochemical) reactions, which vary throughout the course of the year as a result of seasonal variations in the solar zenith distance and for other reasons.

Extensive data on twilight observations (about 100 cases) have been collected at the Blue Hill Observatory near Boston (USA). The day-sky brightness was measured in the vertical of the Sun at an elevation of 20° above the horizon. Five light filters were used in the 0.38-0.68μ region. It was established that the absolute value of the brightness, the gradient, and the color varies as a function of season. In the opinion of the author of [28], the seasonal variations are in part caused by variations in the ozone content. Reference [28] reports that the variations in the ozone content can be calculated from measured values of the twilight sky brightness made through green, orange and red light filters "with surprising accuracy". However, according to [28], the primary cause of seasonal variations in twilight is variations in the scattering of light by aerosol particles at 10-30 km. The vertical distribution of the concentration of aerosols, as obtained from twilight observations in the fall and winter, is in good agreement with the data obtained from direct measurements of the aerosol distribution, using an impactor lifted by a stratosphere balloon, and from optical measurements with rockets. /82

TABLE 14.

$Z_\odot$ \ Z	+75°	+60°	+45°	+30°	0°	−30°	−45°	−60°	−75°
90°.0	11.9	5.19	2.52	1.62	1	1.29	1.73	2.72	3.90
.5	11.4	5.01	2.43	1.54	1	1.27	1.70	2.63	3.68
91.0	11.3	4.92	2.56	1.55	1	1.28	1.70	2.59	3.54
.5	11.6	5.06	2.61	1.55	1	1.36	1.73	2.54	3.43
92.0	11.1	4.87	2.54	1.55	1	1.28	1.69	2.36	2.74
.5	11.0	4.91	2.51	1.55	1	1.26	1.62	2.30	2.55
93.0	11.1	4.98	2.53	1.52	1	1.26	1.56	2.02	2.12
.5	11.2	4.96	2.60	1.53	1	1.24	1.51	1.87	1.88
94.0	11.3	4.89	2.60	1.55	1	1.21	1.45	1.70	1.64
.5	11.6	4.96	2.63	1.58	1	1.19	1.38	1.56	1.44
95.0	12.6	5.27	2.73	1.60	1	1.17	1.35	1.51	1.33
.5	13.8	5.65	2.85	1.59	1	1.13	1.32	1.44	1.31
96.0	15.4	6.27	3.03	1.72	1	1.09	1.24	1.41	1.48
.5	18.0	6.80	3.13	1.77	1	1.08	1.15	1.39	1.60
97.0	23.0	7.76	3.25	1.81	1	1.07	1 15	1.42	1.72
.5	23.1	8.56	3.38	1.86	1	1.11	1.19	1.58	2.14
98.0	26.5	9.35	3.43	1.89	1	1.17	1.23	1.67	2.66

The aforementioned variations occur not only as a function of the time of the year, but also as a function of the phase of the cycle of solar activity and the time of the day. The influence of solar activity on the spectral brightness of the twilight sky is almost uninvestigated (this statement does not refer to the intensity of individual lines and bands in the twilight illumination of the atmosphere, a type of illumination that will be examined in the third part of the present survey). The dependence on the time of the day will be examined in the following section.

2.6. Diurnal Variations in the Spectrophotometric Characteristics of the Twilight Sky.

A comparison of the morning and evening twilight curves definitely shows marked differences between them, the nature of which depends, obviously, on the examined portion of the spectrum, region of the sky, and time of the year.

A typical evening twilight curve (for 0.63μ) is shown in Figure 13; this curve, which covered 32 evenings, was plotted from measurements made in Czechoslovakia [25]. If we compare the evening measurements made at the Abastumani Observatory for 0.64μ (Table 15) with this evening curve, a good agreement can be noted between these data. However, the Abastumani measurements were made at the same time of the morning, a fact that permits the variations from evening to morning to be directly traced. Pertinent in this respect /83

TABLE 15.

Month / $Z_\odot$	Aug.	Sept.		Oct.	Nov.		Dec.	Feb.	March		July		Aug.	
	even	morn	even	even	morn	even	even	even	morn	even	morn	even	morn	even
95°.0	3.96	4.20	3.92	3.81	3.15	3.71	3.80	3.66		3.74		3.57	3.56	3.63
.6	3.64	3.96	3.68	3.54	2.94	3.39	3.60	3.35		3.31	3.55	3.25	3.32	3.32
96.0	3.42	3.78	3.43	3.33	2.75	3.06	3.45	3.05		3.04	3.20	3.01	3.10	3.15
.6	3.16	3.52	3.15	3.06	2.50	2.74	3.21	2.63	3.58	2.70	2.85	2.72	2.83	2.90
97.0	2.96	3.35	2.96	2.87	2.28	2.52	3.04	2.34	3.28	2.47	2.66	2.56	2.60	2.68
.6	2.69	3.09	2.69	2.62	1.99	2.25	2.80	1.93	2.88	2.32	2.42	2.26	2.44	2.37
98.0	2.50	2.90	2.50	2.43	1.74	1.98	2.65	1.71	2.59	1.91	2.20	2.06	2.27	2.19
.6	2.24	2.63	2.26	2.17	1.42	1.73	2.34	1.39	2.17	1.61	1.97	1.82	1.98	2.01
99.0	2.05	2.45	2.10	1.97	1.22	1.54	2.14	1.21	1.82	1.41	1.78	1.65	1.76	1.82
.6	1.80	2.23	1.86	1.71	0.96	1.23	1.83	0.99	1.53	1.17	1.56	1.42	1.55	1.58
100.0	1.62	2.10	1.69	1.53	0.85	1.08	1.60	0.87	1.32	1.09	1.37	1.18	1.40	1.40
.6	1.32	1.85	1.44	1.24	0.68	0.90	1.28	0.68	1.05	0.80	1.06	1.06	1.15	1.17
101.0	1.09	1.72	1.26	1.05	0.62	0.72	1.10	1.55	0.86	0.67	0.85	0.88	0.93	1.00
.6	0.78	1.43	1.01	0.82	0.52	0.62	0.91	0.41	0.63	0.53	0.60	0.73	0.70	0.80
102.0	0.60	1.26	0.97	0.68	0.44	0.55	0.78	0.33	0.46	0.45	0.41	0.59	0.51	

also are the measurements made in India [26], using interference light filters centered at wavelengths of 0.63 and 0.56 ; the results are given in absolute units (candles/cm^2 sterad). Table 16 gives averaged values for the zenith during November and January for the evening (39 observations) and the morning (37 observations) separately. The resulting data were subjected to analysis to clarify the effect of multiple scattering.

Systematic measurements were made in Czechoslovakia of the morning and evening twilight curves at several wavelengths [27]. Table 17 (Lomnitskiy, 49°N, 20°E) and Table 18 (Yavorina, 48°N, 19° E) show measurements in the green portion of the spectrum (0.58μ) in relative units, averaged during August 1956. Simultaneously, observations were made at three wavelengths at the same time, viz., 0.56, 0.59, and 0.63μ at two different stations in Czechoslovakia. The results are shown in relative units for Sitno (48° N, 18°E) in Table 19 and for Ondrzheiova (50° N, 15° E) in Table 20.

It is necessary to bear in mind that these studies of the Czechoslovakian astronomers [27], as well as the other studies mentioned above, used interference light filters characterized by comparatively narrow transmission bands.

TABLE 16.

/84

Z / $Z_\odot$	morning		evening	
	0.63 μ	0.56 μ	0.63 μ	0.56 μ
89°	—	—	9.732×10^{-5}	—
90	5.246×10^{-5}	—	7.193×10^{-5}	—
91	3.069×10^{-5}	5.166×10^{-4}	4.092×10^{-5}	—
92	1.649×10^{-5}	3.299×10^{-4}	2.333×10^{-5}	4.303×10^{-4}
93	7.161×10^{-6}	1.451×10^{-4}	9.719×10^{-6}	1.982×10^{-4}
94	2.621×10^{-6}	4.923×10^{-5}	3.964×10^{-6}	7.737×10^{-5}
95	9.271×10^{-7}	1.662×10^{-5}	1.374×10^{-6}	2.494×10^{-5}
96	3.260×10^{-7}	6.202×10^{-6}	3.676×10^{-7}	8.696×10^{-6}
97	1.151×10^{-7}	2.270×10^{-6}	1.685×10^{-7}	3.205×10^{-6}
98	4.604×10^{-8}	8.056×10^{-7}	7.033×10^{-8}	1.250×10^{-6}
99	2.398×10^{-8}	3.005×10^{-7}	3.261×10^{-8}	$4.540\cdot10^{-7}$
100	1.758×10^{-8}	1.260×10^{-7}	2.174×10^{-8}	1.854×10^{-7}
101	—	$6.317\cdot10^{-8}$	1.790×10^{-8}	8.632×10^{-8}
102	—	3.696×10^{-8}	—	4.418×10^{-8}
103	—	2.474×10^{-8}	—	2.813×10^{-8}
104	—	1.944×10^{-8}	—	2.110×10^{-8}
105	—	1.803×10^{-8}	—	1.835×10^{-8}
106	—	1.694×10^{-8}	—	1.726×10^{-8}
107	—	1.651×10^{-8}	—	1.698×10^{-8}
108	—	1.648×10^{-8}	—	—

These light filters were centered at wavelengths characterized by the fact that the bright lines of emission in the atmosphere are located there: the green (0.557μ) and red (0.630μ) lines of atomic oxygen and the yellow doublet of sodium (0.5893μ). The interpreta-

TABLE 17.

$Z_\odot$	1956 August	
	morn	even
95°.0	−1.03	−0.92
.6	1.34	1.31
96.0	1.51	1.54
.6	1.87	1.86
97.0	2.07	2.10
.6	2.40	2.43
98.0	2.60	2.63
.6	2.87	2.88
99.0	3.01	3.05
.6	3.26	3.28
100.0	3.36	3.44
.6	3.56	3.61
101.0	3.70	3.75
.6	3.92	3.98
102.0	4.04	4.12
.6	4.25	4.32
103.0	4.38	4.41
.6	4.52	

TABLE 18.

$Z_\odot$	morn	even
95°.0	1.06	−1.28
.6	1.33	1.59
96.0	1.55	1.81
.6	1.87	2.14
97.0	2.09	2.36
.6	2.43	2.70
98.0	2.64	2.87
.6	2.92	3.18
99.0	3.10	3.36
.6	3.34	3.60
100.0	3.47	3.73
.6	3.70	3.96
101.0	3.82	4.11
.6	4.01	4.28
102.0	4.12	4.37
.6	4.26	4.51
103.0	4.38	4.57
.6	4.56	4.69

tion of these observations must be made cautiously. The point is that these light filters transmit so much light from the sky (background) that the measured intensities can only be approximately ascribed to the atomic emission lines. For this latter purpose, more /85
reliable results are given by measurements made with spectrographs (these will be discussed in the third part of the survey). But to ascribe the measured intensities primarily to scattered light is also risky, since the brightness of the lines may be a substantial part of the total brightness.

TABLE 19.

$Z_\odot$	0.56 μ		0.59 μ		0.63 μ	
	morn	even	morn	even	morn	even
1	2	3	4	5	6	7
95°.0	+0.92	+0.65	+0.14	+0.11	+0.28	+0.02
.6	0.55	0.29	−0.18	0.49	−0.05	−0.29
96.0	0.30	0.05	0.31	0.73	0.27	0.51
.6	−0.07	−0.33	−0.85	+1.09	−0.67	−0.85
97.0	0.32	0.57	1.10	1.31	0.89	1.10
.6	0.72	0.95	1.45	1.68	1.22	1.44
98.0	0.97	1.17	1.66	1.89	1.42	1.62
.6	1.22	1.43	1.99	2.18	1.73	1.92
99.0	1.43	1.58	2.20	2.36	1.91	2.13
.6	1.66	1.81	2.14	2.60	2.19	2.36
100.0	1.79	1.92	2.58	2.75	2.34	2.50
.6	1.98	2.11	2.81	2.90	2.58	2.72
101.0	2.18	2.22	2.92	3.02	2.74	2.83
.6	2.30	2.33	3.06	3.17	2.92	2.99
102.0	2.39	2.45	3.13	3.27	2.98	3.07
.6	2.52	2.57	3.26	3.34	3.15	3.16
103.0	2.57	2.63	3.31	3.38	3.21	3.22
.6	2.58	2.77	3.37		3.26	3.30

The variation in the spectral composition of the atmospheric twilight glow from morning to evening, which can be ascertained by comparing the twilight curves as measured with various light filters (see Tables 14-19), can also be investigated by comparing the energy spectra of the morning and evening twilights. Such studies were carried out in the Crimea with the use of a fast f:1 GOI spectrograph. Figure 14 shows curves of the intensity as a function of the height of the "twilight beam", i.e., the height of the effective scattering layer, which somewhat exceeds the height of the Earth's shadow (by roughly 20 km for the examined region of the spectrum and which consequently increases with increasing solar zenith distance. These curves show a blueing of the twilight sky at the zenith with increasing solar zenith distance; the curves are plotted such that, for all h, the brightness of the twilight sky for 0.60 is arbitrarily taken as the unit.

The graphs show that the general nature of the variation in color of the sky as a function of the solar zenith distance is identical in the morning and in the evening, but the quantitative characteristics of the variation in color differ somewhat.

TABLE 20.

/86

$Z_\odot$	0.56 μ		0.59 μ		0.63 μ	
	morn	even	morn	even	morn	even
1	2	3	4	5	6	7
96°.0	—14	—16	—0.92	—0 95	—0.65	—0.71
.6	0.45	0.42	1.26	1.29	0.99	1.04
97.0	0.69	0.66	1.49	1.51	1.22	1.27
.6	1.15	1.00	1.82	1.85	1.53	1.59
98·0	1.26	1.21	2 03	2.07	1.73	1.81
.6	1.54	1.50	2.33	2.38	2.03	2.12
99.0	1.70	1.72	2.52	2.56	2.20	2 27
.6	1.94	1.97	2.76	2.80	2.47	2.54
100 0	2.10	2.12	2.92	2.95	2.63	2.68
.6	2.32	2 33	3 13	3.15	2 87	2.90
101.0	2.46	2.48	3.26	3.25	3.02	3.02
.6	2 64	2.64	3 42	3.40	3.22	3.18
102.0	2.73	2 72	2 52	3.47	3.32	3.27
.6	2.84	2.83	3.62	3.52	3.46	3.41
103.0	2.88	2.90	3.67	3.63	3.54	3.48
.6	2 97	3.00	3.73	3.69	3.63	3.56
104.0	2.99	3 04	3.76	3.72	3.68	3.60
.6	3.02	3.09	3.78	3.73	3.72	3.63
105.0	3.04	3.10	3 79	3.73	3.74	3.64
.6	3.04	3.11	3.81	3.74	3·76	3.66

3. MEASUREMENTS OF THE INTENSITY OF INDIVIDUAL LINES OF THE TWILIGHT SKY GLOW.

In addition to the Sun's light scattered by the atmosphere, the characteristics of which were examined in the second part of

this survey, the twilight sky glow includes a number of lines and bands caused by the emission of atoms and molecules that form the Earth's atmosphere. In the visible part of the spectrum, the lines of atomic oxygen and sodium are most intense. In addition, there are hydroxyl OH bands, but their intensity is small and subject to great fluctuations. Even less regular are the spectrograms of the ionized N_2^+ band (about 3914 Å), the lines of other elements of the alkali metal groups (lithium, potassium) as well as the lines of helium and ionized calcium. Data are given below on the intensity and space-time variations of these lines.

3.1. The Emission of Atomic Oxygen.

The red lines of oxygen at 6300 Å and (even weaker) at 6364 Å appear regularly on spectrograms of the twilight sky; the third component of this triplet, the line at 6392 Å is very weak and is observed with difficulty. The intensity of the 6300 Å line is measured at hundreds of Rayleighs and may reach a maximum of 1550 Rayleighs [31]. It slowly decreases with increasing zenith distance of the sun and is reduced gradually to the night value of 50-100 Rayleighs. The intensity of the 6364 Å line reaches 400 Rayleighs and decreases at night to 40 Rayleighs. The width of the 6300 Å line is 0.3 Å, as was shown by interference measurements [32, 33].

There is a diurnal and a seasonal trend in the intensity of the /87
red oxygen lines. It has been established that the evening intensity is greater than the morning intensity [29, 30]. According to the data of the Abastumani Observatory, the ratio between the morning and the evening intensities has a seasonal trend with a minimum in March and September. The intensity of the lines varies throughout the course of the year, having a maximum and minimum in the winter.

As regards the green 5577 Å oxygen line, it was unclear for a long time whether the intensification of the emission was comparable at twilight with that of night emission. Observations, made during the IGY, showed that a twilight intensification of the green line occurred, but was not so regular and marked as the intensification of the red lines [34]. It is apparent that there is a seasonal trend in the brightness of the green line with a maximum in the fall and winter. Observations at the Abastumani Observatory indicate that the greatest twilight intensification of the green line occurs in September-October.

Studies at the Institute of Atmospheric Physics of the Academy of Sciences, USSR established the presence in the twilight glow of the 8446 Å oxygen line ($3^3P - 3^3S_1^0$) with a mean intensity of 13 Rayleighs. Results obtained on the basis of observations at the Zvenigorod Station [36] of the Institute of Atmospheric Physics during 1960 are given in Table 21, where the conditions of observation are shown (Δ is the maximum angle of the Sun's depression below the horizon, h_{min} and h_{max} are the minimum and maximum eleva-

tions of the boundary of the unilluminated part of the atmosphere during the course of an exposure).

Jones and Harrison [37] detected the $^1\Delta g - {}^3\Sigma g$ oxygen band (0.1) at about 1.58μ in the infrared spectrum of the twilight sky. The band showed up on the spectrogram of the evening twilight; this band did not appear in the morning twilight. Measurements made in January - February 1957 showed the brightness of the band to be 17.6 kilorayleighs on the average, varying between 12 and 20 kilorayleighs.

3.2. The Yellow Sodium Doublet.

The twilight flare-up of the 5890 Å and 5896 Å sodium lines is characterized by great brightness, but distinguished from the twilight glow of the red oxygen lines by their short duration. Figure 15 shows examples of the curves of the change in the intensity of the sodium lines as a function of the solar zenith distance. The maximum brightness of the yellow line is observed for a solar zenith distance of 96-98°, when the brightness exceeds the night value by a factor of 10^2 - 10^3. The energy brightness of the lines reaches $5 \cdot 10^{-3}$ erg/sec cm^2 sterad [34]. According to measurements made at the high-altitude station at Andakh [31], the twilight intensity of the sodium doublet is 6000 Rayleighs, which is 250 times greater than the night intensity. According to measurements made in Australia and the Antarctic [38] the twilight intensity exceeds the night intensity by a factor of 15-50.

During the course of the year, the intensity of the twilight sodium illumination varies by a factor of 5-15, according to the measurements of a number of investigators. The maximum is observed in the winter and the minimum, in the summer. However, measurements made in different months and different years yield results that are not in complete agreement. Reference [50] noted that in France, from November to April, the yellow line is clearly observed for a solar zenith distance between 96°30' and 100°; from the beginning of April, the brightness of the line decreases, starting with small solar zenith distances. /88

In June and July, no illumination is observed; it appears in August at a solar zenith distance of 98-100°. At the beginning of October, the yellow line is clearly visible in the spectrograms and its intensity increases in November. In Norway, a clear maximum in the brightness is noted in December-January [51]. According to the data of [52], the emission is not bright in the summer, but very strong in the winter; in fall and spring, the emission is very weak or completely nonexistent. The principal maximum is observed in December, while the secondary maximum is noted in July. The ratio between the winter brightness and the summer brightness is about 3.7 on the average for a solar zenith distance of 95-96°. According to observations made in Canada [50], a clear maximum of $34 \cdot 10^7$ photon/cm^2 sec·sterad occurs at the end of February and a pronounced minimum of $7 \cdot 10^7$ photon/cm^{2}sec·sterad occurs at the end

of June. But studies made in France using a different method [53] recorded intensity maxima in November and March and minima in January-February.

TABLE 21.

Date, 1960	intensity (Rayleigh)	exposure	max angle depression of sun	minimum km	maximum km
15—16 May	10	3 hac. 25 min	15° 30	120	175
26—27	12	2 „ 50 „	13 20	100	135
27—28	15	3 „ 00 „	13 05	100	130
29— 0	14	2 „ 40 „	12 40	100	125
30—31	12	2 „ 30 „	12 30	100	120
5—6 June	17	1 „ 55 „	11 50	100	115
8—9	11	2 „ 30 „	11 30	100	110
10—11	25	2 „ 00 „	10 30	90	100
17—18	16	1 „ 40 „	10 50	85	95
18—19	14	1 „ 25 „	10 50	85	95
20—21	13	1 „ 20 „	10 50	85	95
26—27	15	1 „ 45 „	10 55	85	95
27—28	19	1 „ 40 „	11 00	85	100
4—5 July	11	1 „ 45 „	11 30	90	105
9—10	23	2 „ 00 „	12 00	100	115
10—11	9	2 „ 00 „	12 05	100	115
11—12	14	2 „ 00 „	12 10	100	115
21—22	9	2 „ 40 „	13 40	110	145
24—25	4	3 „ 15 „	14 20	120	155
25—26	8	3 „ 15 „	14 40	130	160
6—7 Aug.	6	3 „ 00 „	17 20	140	210

Unusual spatial variations in the twilight sodium emission have been noted in France [54]; the brightness to the west was 1.5 times greater (on the average) than to the east of the Upper Provence Observatory. However, this relationship may vary during the course of the day.

The ratio of the intensities of the sodium doublet components was determined. According to measurements made near Moscow [39], the ratio $C = J_{d_2} : J_{d_1}$ varies from 1.10 to 1.32 as a function of the solar zenith distance and the point of the sky observed. Measurements in Canada yielded the following: $c = 1.50 \pm 0.02$, while measurements made in France yielded 1.6 ± 0.3 for the morning twilight and 1.4 ± 0.3 for the evening twilight.

3.3. Other Elements in the Alkali Metal Group. /89

The resonance line of lithium (6706.86 Å) was detected in the twilight glow in 1958 at the Abastumani Observatory [42, 43] and, independently, in other places [34]. Attempts were made to determine the ratio of the intensities of the lithium and sodium lines (the yellow doublet). Some determinations gave a ratio on the order of 1:10. However, it should be kept in mind that the intensity of the lithium line is subject to much greater fluctuations than the intensity of the yellow doublet. Prolonged periods are ob-

served, when the lithium line does not appear at all on the spectrograms. The appearance of lithium atoms in the atmosphere may in part be a result of man-made explosions on Earth. In 1959, a report was published regarding the detection of resonance potassium lines at 7664.9 and 7699.0 Å in Norway [44]. These lines occurred in the region of strong atmospheric absorption by the oxygen band (0.0) of the so-called "atmospheric" system, which has a complex structure. This is a great hinderance to a reliable detection of the aforementioned potassium lines. Further systematic studies are necessary.

3.4. Hydroxyl Emission.

In the infrared region of the spectrum of the night-sky emission, the hydroxyl bands are very intense [34], but no bands of this molecule were detected in the spectra of the twilight sky for a long time. In recent years, some bands have been discovered. On the basis of observations made at the Abastumani Observatory, the lines of the (6.1) and (9.3) hydroxyl bands have been recorded and are listed in Table 22.

TABLE 22.

wavelength	band	wavelength	band
6237 Å	(9,3)	6522 Å	(6,1)
6260	(9,3)	6538	(6,1)
6258	(9,3)	6543	(6,1)
6328	(9,3)	6553	(6,1)
6338	(9,3)	6580	(6,1)
6375	(9,3)	6603	(6,1)
6386	(9,3)		
6467	(6,1)		
6499	(6,1)		

In 1960-1961, a seasonal trend in the intensity of the hydroxyl bands was established from observations made at the Abastumani Observatory: the maximum occurs in November to January with a large secondary maximum in June-July. According to preliminary data from the Abastumani Observatory, the (7.2) hydroxyl band has also been detected in the twilight spectrum; at present, only the *R* and *Q* branches of this band have been observed [47].

3.5. The Ionized Calcium Lines.

A report appeared [45] in 1956 to the effect that two rare emission lines with wavelengths at 3933.7 and 3968.5 Å, which corresponds to the wavelengths of the *H* and *K* lines of ionized calcium, were detected on several spectrograms of the twilight sky in Canada. The ratio of the intensities of the lines was equal to 2:1. The spectra were always photographed in such a way that the spectrograph's line of sight intersected the Earth's shadow at a height of

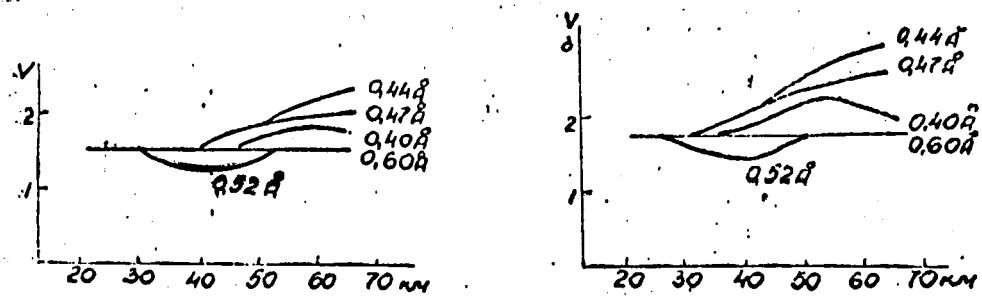

Fig. 14.

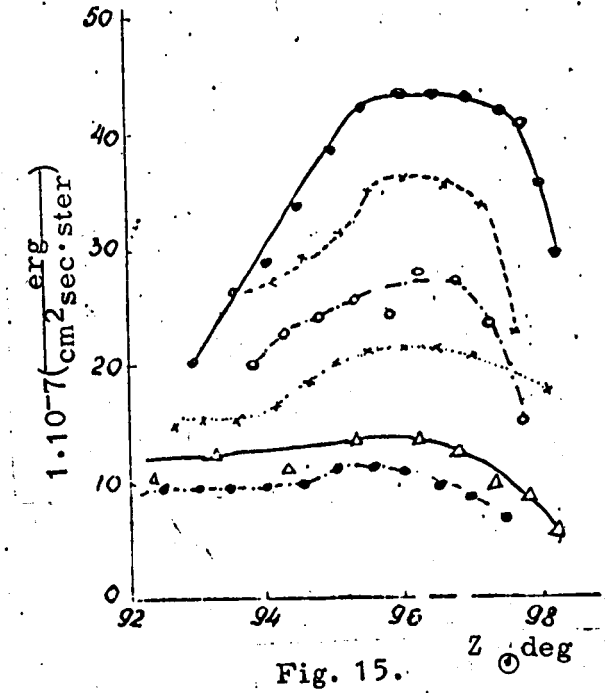

Fig. 15.

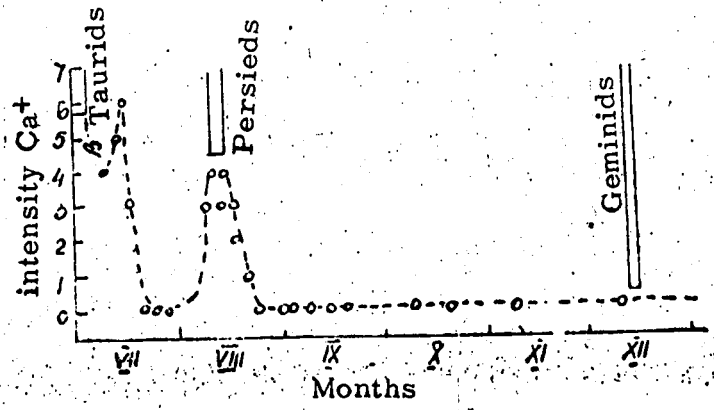

Fig. 16.

100 km. Figure 16 shows how the intensity of the line varied from day to day between July and December. The principal meteor showers are noted in the upper part of the figure. The emission lines disappeared at the end of July and appeared again with greater intensity about the 9-10 of August and persisted daily for about 10 days. After this, the lines disappeared and never reappeared. Similar sporadicity in the appearance of the lines was observed in 1956-1957 also, a fact that provides a basis [45] for supposing that the calcium has meteoric origin. According to the estimates in [45], the maximum areal brightness of the lines was equal to about $2.4 \cdot 10^6$ photons/cm^{2}sec·sterad (about 30 Rayleighs). The sporadic appearance of the *H* and *K* lines of Ca^+ has also been observed by other authors [46]. /91

3.6. The Emission of Nitrogen and Helium.

The band of the negative system of the ionized N_2^+ molecule is observed sporadically in spectra of the twilight sky at about 3914 Å. The intensity of the band usually increases during periods of strong geomagnetic activity [34]. The twilight intensity of the band reaches 800 Rayleighs [31].

The emission of atomic nitrogen is also observed at twilight; occasionally, the spectrograms show a close doublet at 5200 Å [48]. This line is brighter during the evening twilight than during the morning twilight. No relationship with geomagnetic activity has been observed. The intensity of the doublet has been very approximately estimated [31]; values of 30 to 600 Rayleighs have been obtained for the twilight glow and 2 Rayleighs for the night-sky glow.

As a result of studies at the Institute of Atmospheric Physics of the Academy of Sciences, USSR, the emission of helium has been detected on a line at 10830 Å [49]. Research on this intense emission of the upper atmosphere is continuing.

REFERENCES

1. Fesenkov, V.G.: O stroyenii atmosfery (fotometricheskii analiz sumerek). (The Structure of the Atmosphere [A Photometric Analysis of Twilight]). Trudy Glavnaya astrofiz. obs., No. 2, 1923.
2. Shtaude, N.M.: Fotometricheskiye nablyudeniya sumerek kak metod izucheniya verkhnoy atmosfery. (Photometric Observations of Twilight as a Method of Studying the Upper Atmosphere). Trudy komisii po izucheniyu stratosfery pri AN SSSR, No. 1, 1936.
3. Rozenberg, G.V.: Sumerki (Twilight), Moscow, 1963.
4. Khvostikov, I.A.: Vysokiye sloi atmosfery. (The Upper Layers of the Atmosphere). Leningrad, Gidrometeoizdat, 1964.
5. Brunner, W.: Publ. der Eidgenössischen Sternwarte in Zürich (Publications of the Federal Observatory at Zurich), Vol. 6, 1935. In: Beiträge zur Photometrie des Nachthimmels, unter besonderer Berücksichtigung des Zodiakallichtes und der Dämmerungerscheinungen. (Contributions to the Photometry of the Night Sky, with Particular Emphasis on the Zodiacal Light and Twilight Phenomena).
6. Sharonov, V.V.: Doklad. AN SSSR, No. 42, p. 310, 1947: Trudy yubileinoy nauchnoy sessii Lengingrad gosodar'stvennoy universiteta, p. 47, 1948.
7. Kucherov, N.I.: Izv. AN SSSR, ser. geograf. i geofiz., No. 6, p. 465, 1947.
8. Khvostikov, I.A., Ye. N. Magid and A.A. Shubin: Izv. AN SSSR, ser. geograf. i geofiz., No. 5, 1940.
9. Megrelishvili, T.G.: Dokl. AN SSSR, Vol. 53, No. 2, p. 127, 1946.
10. Megrelishvili, T.G.: Byull. Abastum. astrofiz. obs., No. 9, pp. 1-142, 1948.
11. Ashburn, E.V.: J. Geophys. Res., Vol. 57, No. 1, p. 85, 1952.
12. Shtaude, N.M.: Izv. AN SSSR, ser. geogr. i geofiz., Vol. 13, No. 4, p. 307, 1949.
13. Hulburt, E.O.: J. Opt. Soc. Amer., Vol. 28, No. 7, p. 227, 1938.
14. Darchiya, A.Kh.: Izv. Glav. astrofiz. obs., AN SSSR, No. 165, 1960.
15. Barteneva, O.D. and A.N. Boyarova: Trudy Glav. geofiz. obs., No. 100, p. 133, 1960.
16. Ljunhall, A.: The Intensity of Twilight and its Connection with the Density of the Atmosphere. Meddelande Fran Lunds Astronom. Observ. Ser. 11, No. 125, 1949.
17. Dave, J.V. and Ramanathan: Proc. Indian Acad. Sci, Vol. A 43, No. 2, pp. 67-68, 1956.
18. Divari, N.B.: Geomagnetizm i aeronomiya, Vol. 11, No. 4, 1962.
19. Volz, F.E. and R.M. Coody: The Intensity of Twilight and Upper Atmospheric Dust. J. of Atmosph. Sci., Vol. 19, No. 5, p. 385, 1962.

20. Gadsden, M.J.: Atmosph. and Terr. Phys., Vol. 10, No. 3, p. 176, 1957.
21. Divari, N.B.: Dokl. AN SSSR, Vol. 122, No. 5, p. 795, 1958.
22. Hulbert, E.O.: J. Opt. Soc. Am. Vol. 43, No. 2, p. 113, 1953.
23. Yarin, V.I.: V sb: Polyarniye siyaniya i svecheniye nochnogo neba. (Aurorae and Illumination of the Night Sky). Rezul'taty MGG, Vol. 1, No. 9, 1962.
24. Gnilovskiy, Ye.V. Ob infrakrasnom spektre sumerechnogo neba. (The Infrared Spectrum of the Twilight Sky). Vestnik Leningr. univ., ser. fiz. i khim., No. 4, Issue 1, 1964.
25. Link, F., L. Neuzil and I. Zacharov: Astronom. Inst. Czechosl. Akad. Sc. Publ., No. 38, 1958.
26. Chiplonkar, M.W. and P.V. Kulkarni: Further Studies of the Twilight Illumination. Byul. astron. institutov Czechoslovakia, Vol. 9, No. 4, pp. 128-132, 1958.
27. Link, F., L. Neuzil and I. Zacharov: Astronom. Inst. Czechosl. Acad., Sc. Prague. Ondrejov. Publ., No. 38, 1958.
28. Volz, F.: Stratosphärische Trübung und Ozongehalt nach Dämmerungsmessungen. Zusammenfassung. (Stratospheric Turbidity and Ozone Content on the Basis of Twilight Measurements. A Survey). Berichte des deutschen Wetterdienstes, Vol. 12, No. 91, p. 150, 1963.
29. Elvey, C.T. and A.H. Farnsworth: Spectrophotometric Observations of the Light of the Night Sky. Astrophys. J., Vol. 96, No. 3, pp. 451-467, 1942.
30. Link, F.: Aurorae and Airglow. Internat. Geophys. Year and Cooperation in Czechoslovakia 1957-1959. Prague, Czech. Acad. of Sciences, pp. 95-111, 1960.
31. Blackwell, D.E., M.F. Ingham and H.N. Rundle: Observations of Twilight and Night Sky Airglow Near the Equator. Ann. geophys., No. 1, pp. 150-151, 1960.
32. Wark, D.Q.: A Determination of the Line Width of the λ 6300 Å of Oxygen in the Twilight Sky. Nature, No. 178, pp. 689-691. 1956.
33. Philipps, H.: The Determination of the Widths of the Airglow and Twilight Flash. In: The Airglow and the Aurorae. A Symposium Held at Belfast in September 1955. Eds. E.B. Armstrong and A. Dalgarno. Suppl. J. Atmos. and Terr. Phys., Vol. 5, pp. 67-72, 1956.
34. Khvostikov, I.A. Fizika ozonosfery i ionosfery. (Physics of the Ozonosphere and Ionosphere). Izd. AN SSSR, Moscow, 1963.
35. Chamberlain, John: Physics of the Aurorae and Illumination of the Atmosphere. 1963.
36. Shefov, N.N.: Sumerechnaya emissiya 8466 Å. (Twilight Emission of the 8466 Å). Collection: Polyarniye siyaniya i svecheniye nochnogo neba, Izd. AN SSSR, No. 9, pp. 55-58, 1962.
37. Jones, A.A. and A.W. Harrison: Infrared Emission Band in the Twilight Airglow Spectrum. J. Atmos. and Terr. Phys., No. 13, pp. 45-60, 1958.
38. O'Brien, B.J.: Southern Hemisphere Observations of Sodium Emission Throughout Twilight. J. Geophys. Res., Vol. 65, No. 1, pp. 137-140, 1960.

39. Gal'perin, Yu. I.: Otnosheniye intensivnostey komponent zheltogo dubleta natriya v spektre sumerechnogo neba. (Ratio of Intensities of Components of the Yellow Doublet of Sodium in the Spectrum of the Twilight Sky). Astron. Zh., Vol. 33, No. 2, pp. 173-181, 1956.
40. Harrison, A.W. and A.V. Jones: The Intensity Ratio of the D-Lines in Twilight. In: The Airglow and the Aurorae. A Symposium Held at Belfast in September, 1955. Eds: E.B. Armstrong and A. Dalgarno. Suppl. J. Atmos. and Terr. Physics, Vol. 5, pp. 114-121, 1956.
41. Nguyen-Huu-Doan: Rapport des intensités des raies D_2 and D_1 du sodium emisés dan l'atmosphere au crépuscule et pendant la nuit. (Ratio of the Intensities of the D_2 and D_1 Lines of Sodium Emitted in the Atmosphere at Twilight and at Night). Comptes Rendus, Vol. 249, No. 5, pp. 739-741, 1959.
42. Megrelishvili, T.G.: O lyuminestsentsii sumerechnogo neba v infrakrasnoy oblasti spektra. (Luminescence of the Twilight Sky in the Infrared Region of the Spectrum). Dokl. AN SSSR, Vol. 116, No. 5, pp. 766-769, 1957.
43. Khvostikov, I.A. and T.H. Megrelishvili: New Bands and Lines in the Twilight Sky Spectrum. Nature, Vol. 183, No. 4664, p. 811, 1959.
44. Kvifte, G.: Alkaliemetaller i den ovre atmosfaere. (Alkali Metals in the Upper Atmosphere). Fra. Fyzik Verden, Vol. 21, No. 2, pp. 253-265, 1959.
45. Jones, A.V.: Ca II Emission Lines in the Twilight Spectrum. Nature, Vol. 178, No. 1527, pp. 276-277, 1956.
46. Dufay, M.: Étude photoélectrique du spectre du ciel nocturne dans le proche infra-rouge. (Photoelectric Study of the Night-Sky Spectrum in the Near Infrared). Ann. geophys., Vol. 15, No. 2, pp. 134-152, 1959.
47. Megrelishvili, T.G. and T.I. Toroshelidze: Byull. Abastum. astrofiz. obs., No. 29, 1952. Astron. tsirk. No. 197, 1958.
48. Khvostikov, I.A. Svecheniye nochnogo neba. (Illumination of the Night Sky). Izd. AN SSSR, 1948.
49. Shefov, N.N.: Emissiya geliya v verkhney atmosfere. (Helium Emission in the Upper Atmosphere). Collection: Polyarniye siyaniya i svecheniye nochnogo neba. Izd. AN SSSR, Moscow, pp. 50-65, 1962.
50. Bricard, J. and A. Kastler: Recherches sur la radiation D du sodium dans la lumière du ciel crépusculaire et nocturne. (Studies of the D Radiation of Sodium in the Light from the Twilight and Night Sky). Ann. geophys., Vol. 1, No. 1, pp. 1-30, 1944.
51. Vegard, L., G. Kvifte, A. Omholt and S. Larsen: Studies of the Twilight Sodium Lines from Observations at Oslo and Tromso, and Results of Auroral Spectrograms from Oslo. Geophys. Publ., Vol. 19, No. 3, p. 22, 1955.
52. Barber, D.R.: Note on the Seasonal Variation of Sodium D-Line Emission in Twilight. J. Atmos. and Terr. Phys., Vol. 5, No. 5-6, pp. 347-348, 1954.
53. Blamont, J.E.: Observations de l'émission atmosphérique des

raies D du sodium au moyen d'un appareil à balayage magnétique. (Observations of Atmospheric Emission of Sodium D-Lines by Means of a Device for Magnetic Scanning). In: The Airglow and the Aurorae. A Symposium Held at Belfast in September, 1955. Eds.: E.B. Armstrong and A. Dalgarno. Suppl. J. Atmos. and Terr. Phys., No. 5, pp. 99-113, 1956.

54. Blamont, J.E., T.M. Donahue and V.R. Stull: The Sodium Twilight Airglow 1955-1957. Ann. geophys., Vol. 14, No. 3, pp. 253-281, 1958.

55. Megrelishvili, T.G. and T.I. Toroshelidze: K voprosu o variatsiyakh svecheniya natriya v sumerkakh. (The Problem of Variations in Illumination of Sodium in Twilight). Byull. Abastum. Astrofiz. obs., No. 32, p. 165, 1965.

Translated for the National Aeronautics and Space Administration by:
Aztec School of Languages, Inc.,
Research Translation Division (243)
Acton, Massachusetts
NASw-1692